Advances in Water Resources 201 (2025) 104976

Contents lists available at ScienceDirect

Advances in Water Resources

journal homepage: www.elsevier.com/locate/advwatres

Field-scale soil moisture dynamics predicted by deep learning

Sahar Bakhshian [a], Negar Zarepakzad [b], Hannes Nevermann [b,c], Cathy Hohenegger [d], Dani Or [e], Nima Shokri [b,c,*]

[a] Department of Earth, Environmental, and Planetary Sciences, Rice University, Houston, TX 77005, USA
[b] Institute of Geo-Hydroinformatics, Hamburg University of Technology, Hamburg, Germany
[c] United Nations University Hub on Engineering to Face Climate Change at the Hamburg University of Technology, United Nations University Institute for Water, Environment and Health (UNU-INWEH), Hamburg, Germany
[d] Max Planck Institute for Meteorology, Hamburg, Germany
[e] Department of Civil and Environmental Engineering, University of Nevada, Reno, NV, USA

ARTICLE INFO

Keywords:
Soil moisture dynamics
Deep learning
Field measurement

ABSTRACT

Soil moisture plays a critical role in land–atmosphere interactions. Prediction of its dynamics is still a grand challenge. While in-situ measurements using sensors offer highly temporally resolved and accurate information compared to satellite observations, existing sensor networks are sparse and scarce. Here we propose a deep learning model for bridging the gap between infrequent satellite observations and sparse in-situ sensor network to improve near-term soil moisture predictions. The Long Short-Term Memory (LSTM)-based deep learning model was used to forecast soil moisture dynamics using soil parameters and climatic variables (e.g. air temperature, relative humidity, pressure, wind speed, turbulent fluxes, solar and terrestrial waves) collected from a dense network of sensors in a field located in Germany in an area of about 20 hectares. The dynamic time-lagged cross-correlation between soil moisture and other co-located soil and climatic features was calculated and a set of optimal predictors for training the LSTM model was selected. To efficiently learn the long-term dependency of soil moisture on its historical trends and to improve the prediction capability of the model, we optimized the LSTM structure, hyperparameters, and the size of the sliding window based on the goodness of fit (R^2 score) of the model. We also examined the feasibility of employing the model developed using temporal data from one location for the prediction of soil moisture at other locations across the landscape. The results illustrate the robustness and efficiency of the proposed model for the spatio-temporal prediction of soil moisture.

Plain Language Summary

Understanding and monitoring soil moisture dynamics is crucial affecting ecosystem health, climate and extreme weather patterns, and the agricultural sector. However, predicting the temporal and spatial variation of soil moisture is challenging because of the complex interactions between the land and atmosphere. While soil moisture measurement with in-situ ground-based sensors provide a high level of temporal frequency in comparison to satellite data, the implementation of dense monitoring networks to capture spatial variability of soil moisture is not economically viable. To address this problem, we utilized machine learning techniques to predict temporal and spatial variation of soil moisture using data we measured in a field in Germany. The developed model was examined against the experimental data with the results illustrating that AI-based solutions could offer a powerful tool to predict soil moisture dynamics.

1. Introduction

Soil moisture (SM) plays a key role in land–atmosphere interactions (Seneviratne et al., 2010), maintaining the sustainability of dryland ecosystems (Zhang et al., 2017), soil health (Lehmann et al., 2020), soil salinity (Hassani et al., 2021) and carbon cycles via evaporation and transpiration (Shokri et al., 2024; Humphrey et al., 2021; Or et al., 2013; Shokri et al., 2012). Soil moisture normally exhibits a high degree of temporal and spatial variability pertaining to heterogeneity in soil characteristics, topographical features, vegetation types, land use patterns (Jiao et al., 2022), and meteorological conditions (Brocca et al., 2010). This multifactorial dependency causes major challenges to the prediction of soil moisture across various spatiotemporal scales

* Corresponding author at: Institute of Geo-Hydroinformatics, Hamburg University of Technology, Hamburg, Germany.
E-mail address: nima.shokri@tuhh.de (N. Shokri).

https://doi.org/10.1016/j.advwatres.2025.104976
Received 21 April 2024; Received in revised form 30 March 2025; Accepted 31 March 2025
Available online 19 April 2025

and to the observation of soil moisture over large areas. Thus, it is crucial to develop quantitative tools capable of predicting soil moisture variability required to establish a better understanding of the interplay between the environmental processes and soil moisture dynamics. Furthermore, accurate quantification of the spatiotemporal patterns of soil moisture would improve prediction accuracy of climate models as well as the management of extreme events such as drought and flooding (Seneviratne et al., 2010).

Soil moisture can be quantified through in-situ measurements, satellite remote sensing, and hydrological models. Satellite remote sensing technologies offer great potentials to quantify SM globally as illustrated for example by the Soil Moisture Active Passive (SMAP) mission (Entekhabi et al., 2010). However, these technologies can obtain soil properties within the first few centimeters of the soil layer and their measurements are often collected at low spatial and temporal resolution for agricultural and engineering applications. This could be a restricting factor in several applications such as management of small farms, where high resolution data in both time and space and root-zone SM matter. Furthermore, there are limitations in the retrieval of the satellite-based SM in the regions covered with snow, ice, and dense vegetation (Dorigo et al., 2017). On the other hand, in-situ point measurements offer higher spatiotemporal resolutions than remote sensing techniques. However, in-situ measurements are constrained to limited number of selected points and therefore spatially restricted (Brocca et al., 2010).

Given the limitations of the SM measurement techniques and the complexity of the relationship between soil moisture, other soil properties, and meteorological factors, machine learning methods can be used as an effective alternative approach to predict SM at high spatiotemporal resolutions and reveal the correlation between SM and the controlling factors. In addition, with the recent developments in communication technologies within the internet of things (IoTs), continuous collection of large volume of streaming soil and meteorological data using wireless sensor technology is viable (Nagaraj et al., 2021; Chen and Jin, 2012). The large data streams acquired from sensors provides the opportunity for building data-driven predictive models to forecast future trends of soil moisture under different boundary conditions. Machine learning techniques provide a unique opportunity to 'learn' the correlation between the soil moisture and different controlling factors. Several recent studies demonstrated the potentials of this emerging tool in digital soil mapping and predicting soil spatio-temporal properties, such as soil salinity, organic carbon, bulk density, Cation Exchange Capacity (CEC), pH, soil texture fractions and coarse fragments, and soil moisture is no exception (Hengl et al., 2017; Hassani et al., 2021, 2020). Limited studies have implemented data-driven models to predict both temporal and spatial variations in soil moisture dynamics. Teshome et al. developed a deep learning regression model for sub-hourly soil moisture prediction using weather and soil characteristics and compared the prediction capability of their model to traditional models such as eXtreme gradient boosting (XGB), light gradient-boosting (LGB), cat boosting (CB), random forest (RF), k-nearest neighbors (kNN), and long short-term memory (LSTM) (Teshome et al., 2024). Acharya et al. evaluated the performance of different models including classification and regression trees, random forest regression, boosted regression trees, multiple linear regression, support vector regression, and artificial neural networks to predict soil moisture in the Red River Valley of the North using weather station, soil, and crop data (Acharya et al., 2021).

Given the importance of soil moisture prediction and availability of in-situ monitoring data, the objective of this study is to investigate the robustness of deep learning based approaches to forecast the temporal and spatial variability of soil moisture at the field scale. We aim to address:

1- How deep learning techniques can be employed to forecast soil moisture dynamics, while integrating the effects of complex interactions between soil properties and meteorological factors on soil moisture?

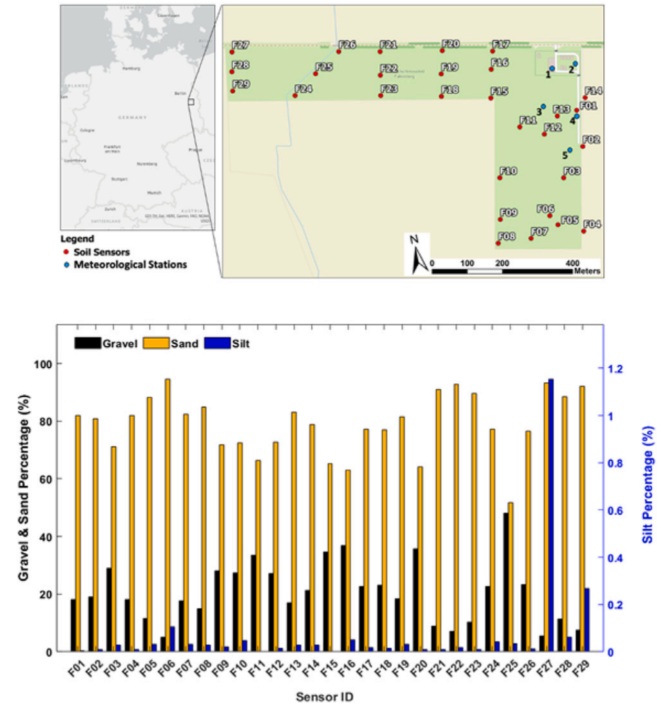

Fig. 1. Top: Location of soil sensors (F01-F29) and meteorological stations (1 and 2) located in Falkenberg, Germany for a monitoring period of 15 months (May 2021–July 2022). Bottom: Particle size distribution of collected soil samples at the location of 29 soil sensors.

2- To what extent the dynamic variability of soil moisture can be predicted using deep learning?

3- Can SM spatial variability observed in one field be predicted using ML models built using in-situ SM data measured only at one location in the same field?

To address these questions, we conducted a field campaign to measure in-situ soil and meteorological data for about one year in a field located in Germany, southeast of Berlin. We then employed a long short-term memory network to "learn" the complex relationship between the target soil moisture and predictor variables. In-situ soil data obtained at one location of the field as well as the meteorological data gathered at one of the climatic stations were used to generate the LSTM model. The model was then validated with evaluating its accuracy for prediction of soil moisture dynamics at other locations containing in-situ soil data, which were not used for building the ML model. The detailed description of the data, methodology, and results and discussion is presented in the following sections.

2. Material and methods

2.1. Study area and data acquisition

The data used in this study were collected from a field in Falkenberg, Germany using in-situ measurements of soil and meteorological properties for a period of 15 months (May 2021–July 2022). Additional information about this field measurement which was a part of a larger campaign, The Field Experiment on Submesoscale Spatio-Temporal Variability in Lindenberg (FESSTVaL), can be found in Hohenegger et al. (2023) . The land cover of this field mainly consists of grass. The dataset related to soil properties consists of soil moisture and soil temperature collected from a network of 29 ground-based sensors in a study area of around 20,000 m^2 (see Fig. 1). Soil moisture and temperature sensors included thermofox manufactured by Scanntronik located in Zorneding, Germany. Soil parameters were recorded with a

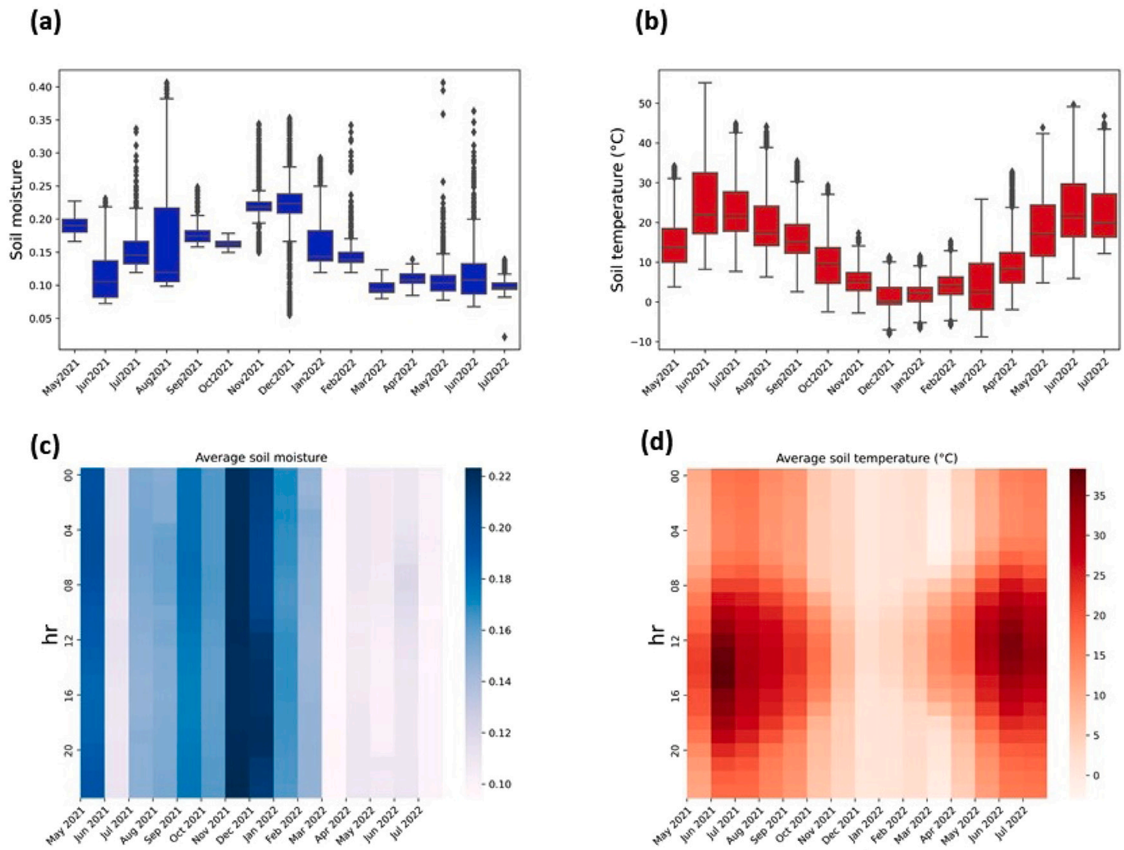

Fig. 2. Monthly variation of soil moisture (a) and soil temperature (b) measured in sensor F01. Hourly variation of soil moisture (c) and soil temperature (d) during day and night averaged over all days in a given month in sensor F01.

temporal resolution of 10 min at 5 cm depth below the soil surface. The sensors detect soil moisture by measuring dielectric permittivity through a capacitive frequency domain technique (Oates et al., 2017) with a frequency of 80 MHz. The permittivity measures were converted into soil water content using Topp's equation (Topp et al., 1980). Thermofox's temperature sensors has a high-precision capability to measure temperatures in the rage of −30 °C to +80 °C with a resolution of 0.1 °C. Figs. 2a and b represent monthly variation of soil moisture and soil temperature measured in one sensor labeled as F01. As can be seen, soil moisture exhibits seasonality variations with higher levels tending to occur in winter, mainly influenced by rainfall events. It can be also observed that soil temperature is negatively correlated with soil moisture. Fig. 2c and d displays the hourly variation of soil moisture and soil temperature during day and night averaged over all days in a given month. According to those heat maps, daily variation of soil temperature is sensible, while soil moisture dynamics is mainly noticeable at the monthly scale, reflecting the fact that variations in soil moisture are controlled by not only the soil-related factors but also by other environmental variables.

To determine the soil texture, soil samples were collected at the location of 29 soil sensors and analyzed their particle size distribution. The size of soil particles was measured using a set of sieves in the range of 50 μm to 2 mm. The experiments consist of mechanically vibrating a soil sample with a known weight for 10 min with an amplitude of 1 mm through a set of sieves with progressively smaller mesh sizes. The weight of grains that remained on each sieve was then measured which was used to determine the particle size distributions with the results presented in Fig. 1. Since the soil texture is almost homogeneous with sandy soil as the main texture in all soil measurement stations, soil texture has not been considered an influential predictor affecting the SM in the predictive ML model built in our investigations.

In addition to soil moisture and soil temperature, meteorological data were collected during the field experiments. The meteorological parameters including air temperature, air humidity, wind speed, precipitation, air pressure, global radiation, reflected radiation, thermal radiation, counter radiation, soil heat flux, shear stress velocity, sensible turbulent heat flux, and latent turbulent heat flux were recorded every 10 min. The duration of the measurements over 15 months provides a dataset covering a wide range of meteorological conditions including dry and hot seasons as well as wet and cold seasons. This comprehensive dataset was used for developing models based on machine learning algorithms capable of predicting SM dynamics under a wide range of boundary conditions. Fig. 3 represents the temporal evolution of soil moisture and soil temperature as well as some of the meteorological factors measured with the sensor F01.

2.2. Deep learning algorithm

Long short-term memory (LSTM) networks were employed to predict high-temporal resolution soil moisture. Through the LSTM algorithm, we are able to capture long-term temporal dependency of soil moisture on the predictors. Long short-term memory (LSTM) is an enhanced recurrent neural network (RNN) architecture, which is well-suited to learning long-term dependencies in sequential data by using memory cells. RNNs typically suffer from the issue of vanishing gradients, which makes it challenging to learn the trend of long sequential data (Bengio et al., 1994; Hochreiter and Schmidhuber, 1997; Bakhshian and Romanak, 2021; Mahdaviara et al., 2022). However, the gating mechanism used in LSTM handles the memorizing process by controlling the communications among various memory units. An LSTM unit is composed of a memory cell (cell state) as well as input, output, and forgetting gates. Through this structure, a controlled flow

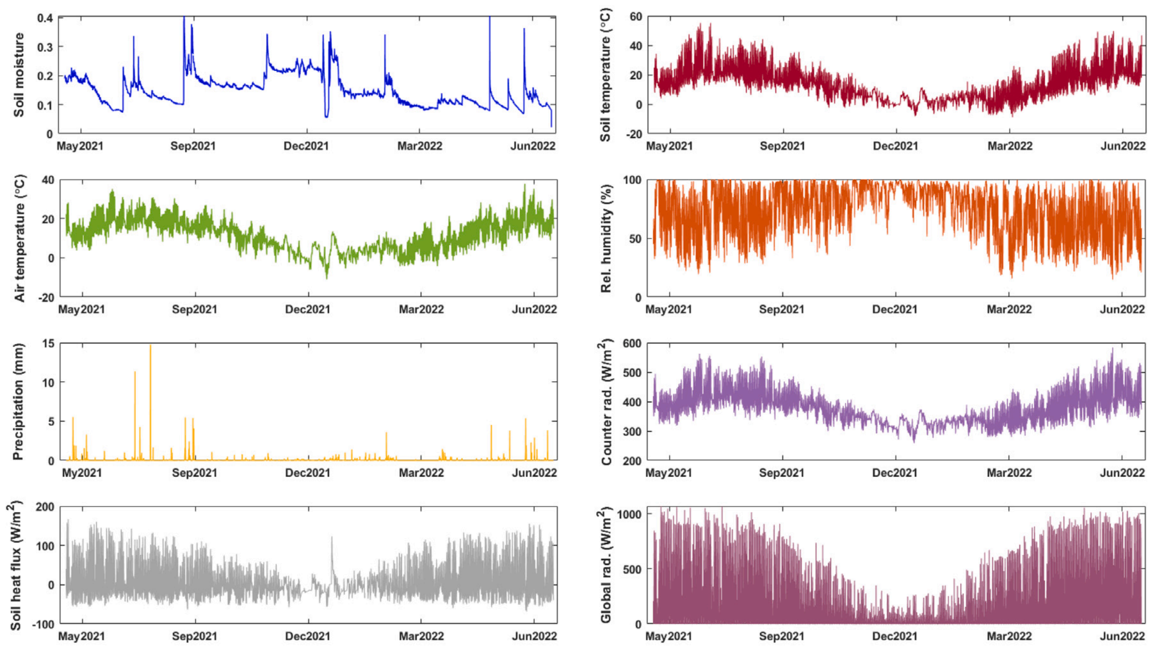

Fig. 3. Original data streams collected through one of the soil sensors (sensor F01) and meteorological station 1. Soil moisture and temperature were obtained using soil sensors and air temperature, relative humidity, precipitation, counter radiation, soil heat flux, and global radiation were measured using meteorological sensors.

of information is created and the forget gate decides on the information that needs to be discarded from the cell state. The information stored in the memory state C_t at the time-step t is controlled by the input gate i_t and a second gate C_t^*. The forget gate f_t determines the extent to which the information should remain in the memory cell. The output gate o_t controls the information flow to be used for computing the output of the LSTM unit. The architecture of an LSTM unit can be described as follows (Gers et al., 2000; Hochreiter and Schmidhuber, 1997):

$$i_t = \sigma(U_i X_t + H_{t-1} W_i + b_i) \tag{1}$$

$$f_t = \sigma(U_f X_t + H_{t-1} W_f + b_f) \tag{2}$$

$$C_t^* = tanh(U_c X_t + H_{t-1} W_c + b_c) \tag{3}$$

$$C_t = f_t \odot C_{t-1} + i_t \odot C_t^* \tag{4}$$

$$o_t = \sigma(U_o X_t + H_{t-1} W_o + b_o) \tag{5}$$

$$H_t = tanh(C_t) \odot o_t \tag{6}$$

where X_t and H_t represent the input and hidden states in the time step t, σ is the sigmoid activation function, W_i, W_f, W_c, W_o, U_i, U_f, U_c, U_o, and b_i, b_f, b_c, b_o are recurrent wights, input weights, and bias terms, respectively. H_{t-1} and C_{t-1} are the hidden and memory state at time-step $t-1$, respectively. $\odot$ refers to point-wise multiplication. The activation function of the neurons in the model is sensitive to the range of the input data. Thus, to minimize the effect of scale disparity and improve the stability and performance of the ML model, the data was normalized using Min–Max normalization. To mitigate overfitting, a dropout layer was introduced within the LSTM layers by removing a portion of weights and reducing the interdependence between the network nodes (Srivastava et al., 2014). The predictive LSTM model was built in Python 3.9 using the deep learning tool Keras, in which TensorFlow was used as the backend (Géron, 2017).

2.3. Model performance evaluation

To test the accuracy of the developed model, five metrics including root mean square error (RMSE), coefficient of determination (R^2), mean absolute error (MAE), and Kling-Gupta Efficiency (KGE) (Gupta et al., 2009) were calculated for the training and test sets, as follows:

$$RMSE = \sqrt{\frac{1}{N}\sum_{i=1}^{N}(Z_i - X_i)^2} \tag{7}$$

$$R^2 = 1 - \frac{\sum_{i=1}^{N}(X_i - Z_i)^2}{\sum_{i=1}^{N}(X_i - \mu_{obs})^2} \tag{8}$$

where Z_i denotes the predicted data stream, μ_{obs} and N are the mean and size of the data stream, respectively.

The KGE is defined as

$$KGE = 1 - \sqrt{(r_p - 1)^2 + (\beta - 1)^2 + (\gamma - 1)^2} \tag{9}$$

where r_p is the Pearson's correlation coefficient, β is the bias ratio (μ_{pred}/μ_{obs}), and γ is the variability ratio ($\sigma_{pred}/\sigma_{obs}$). μ_{pred} (μ_{obs}) and σ_{pred} (σ_{obs}) are the mean and standard deviation of the predicted (observed) data stream. The KGE value of an ideal forecast is 1.

The accuracy of the soil moisture values predicted by the LSTM model was initially evaluated using the model testing phase. The calibrated model for sensor F01 is then used in other locations of the field that contain in-situ data, which are not used for training the LSTM model.

2.4. Network structure characteristics and optimization

The first step for building the ML model is to optimize its architecture including its hyperparameters. The hyperparameters of the LSTM model define the nonlinear degree of the network and thus highly affect the performance of the model. In order to obtain the optimal LSTM network structure, two search methods called grid search (GS) and random search were used for optimizing the hyperparameters and loss function (Abbasimehr et al., 2020; Reimers and Gurevych, 2017). Using

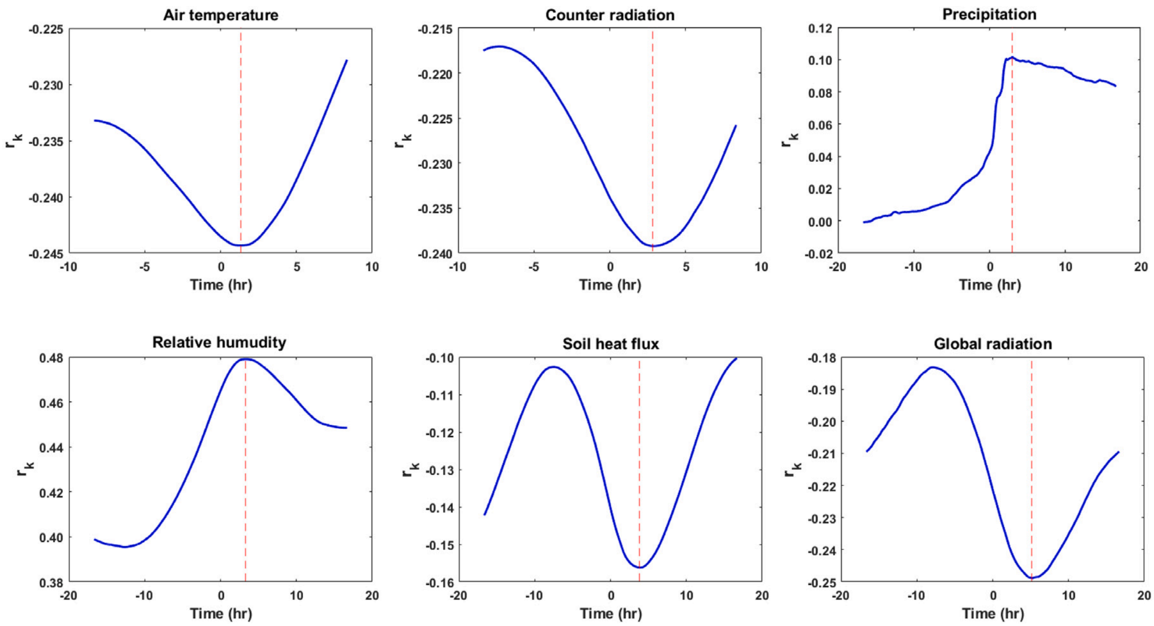

Fig. 4. Time-lagged correlation between soil moisture and air temperature, counter radiation, precipitation, relative humidity, soil heat flux, and global radiation. The peak of synchrony (minimum/maximum r_k) is depicted with red dashed lines.

the GS method, we optimized the batch size, epoch size, optimizer, and activation function. The batch size was varied from 10 to 100 and the best-performing model architecture was achieved with a size of 20. When the number of training epochs is too large, the model may suffer from overfitting, so selecting an optimal epoch size is necessary to achieve a model with strong generalization ability and high performance. The best epoch value for this dataset was found to be 48 with R^2 score used as a criterion to evaluate the prediction performance. Optimizers are functions used to alter the attribute of an ML model such as weights and learning rates to minimize the loss function. In this study, seven optimizers including RMSprop, SGD, AdaGrad, Adadelta, Adam, AdaMax, and Nadam were tested (Sun et al., 2020). According to the GS analysis, we found that the Adam optimizer showed the minimum loss function and required less computational time and memory usage. Another factor that was optimized was the activation function, which controls the data transfer between the layers and imposes nonlinear behavior on the deep learning network. Optimization was conducted by searching for the best activation function among SoftMax, SoftPlus, SoftSign, ReLU, tanh, sigmoid, hard-sigmoid, and linear functions. We found that the most optimal activation function for the LSTM architecture is ReLU, which showed the highest learning rate as a non-saturated activation function (Varshney and Singh, 2021). We also performed random experiments to manually tune the number of layers and neurons as well as the size of the train and test datasets. Compared to the grid search experiments, the random search was found to maintain a more efficient optimization of those hyperparameters and required less computational time (Bergstra and Bengio, 2012). It was found that a single-layer LSTM model with 16 neurons is the best architecture with the minimum loss functions.

Another hyperparameter that is required to be selected effectively is the lag size, which defines the number of past observations to be used for the prediction. The dependencies among the successive observations can be captured with an appropriate time-lag value. A small lag-size value may not transfer sufficient information, while a large value of time lag may increase the model complexity and even reduce its performance (Surakhi et al., 2021). We manually ran different experiments with a varied number of lagged observations and found that a lag size of 8 is the best value that optimizes the performance of the model by generating the lowest error rate.

2.5. *Time-lagged correlation analysis*

The changes in some of the soil and climatic parameters can take some time to noticeably affect soil moisture and be reflected in the measurements. Therefore, the time-lag effect of soil moisture response to other soil and climatic features was analyzed by a time-lagged correlation analysis. The maximum correlation and the corresponding lag time between the time series of soil moisture and that of other features were calculated. Initially, the correlation coefficients between the soil moisture (X) and a given feature (Y) were calculated for different time lags as the following:

$$r_k = \frac{\sum_{i=1}^{n-k}(X_i - \overline{X}_i)(Y_{i+k} - \overline{Y}_{i+k})}{\sqrt{\sum_{i=1}^{n-k}(x_i - \overline{X}_i) \times \sum_{i=1}^{n-k}(Y_{i+k} - \overline{Y}_{i+k})}}, \tag{10}$$

where r_k refers to the correlation coefficient between time series X and Y; k is the time lag; and $\overline{X}$ and $\overline{Y}$ are the average values of time series X and Y. The sign of r_k is representative of the negative and positive correlation between the time series. The sign of the time lag k defines the leader-follower relationship between the soil moisture and any given feature. $k = 0$ represents synchronous changes in soil moisture and a given feature.

3. Results and discussion

3.1. *Correlation analysis*

The correlation coefficient and the lag time between soil moisture and all other soil and climatic features corresponding to the maximum correlation were calculated. Since the goal of the development of the ML model is to predict the soil moisture, the features with a negative time lag (k) of the soil moisture response were selected for building the LSTM model. A negative time lag implies that changes in a given variable precede changes in the soil moisture. In other words, the input features to the LSTM model were chosen such that the response of the soil moisture variations were lagged behind the changes in those features. When calculating the time-lagged correlation between soil data taken from sensor F01 as well as climatic data taken from the meteorological station 1 (see Fig. 1), the list of features with negative time delay with respect to the soil moisture are found to be

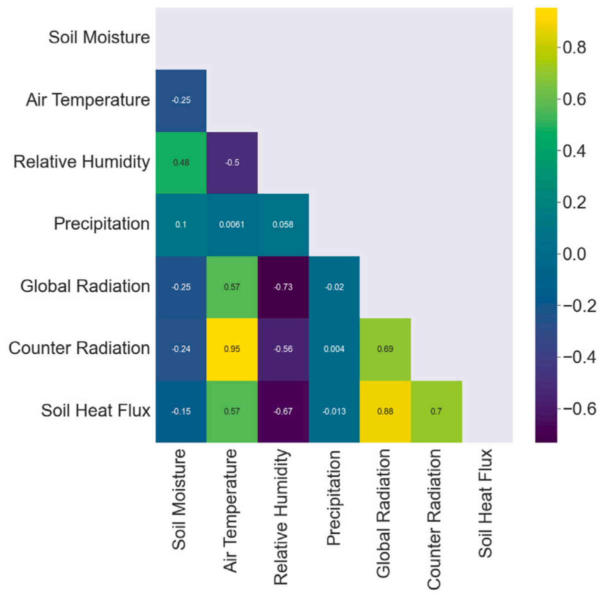

Fig. 5. Pearson's correlation analysis between soil moisture, air temperature, precipitation, counter radiation, relative humidity, soil heat flux, and global radiation. Time series were shifted in time with their respective time lags to achieve maximum correlation with soil moisture.

air temperature, precipitation, counter radiation, relative humidity, soil heat flux, and global radiation.

The time-lag correlation between the soil moisture and those features are displayed in Fig. 4. In average, the smallest and largest time lag was found to correspond to the soil moisture response to air temperature and global radiation, respectively. According to the results (Fig. 4), soil moisture was affected by the changes in the soil/air temperature, counter radiation, and precipitation within the preceding 3 h. While the soil moisture response to other factors (*e.g.* humidity, soil heat flux, and global radiation) occurred with longer time lags up to 5.16 h. As can be seen, there are negative correlations between soil moisture and air temperature, counter radiation, soil heat flux, and global radiation. In contrast, the correlation between soil moisture and precipitation and relative humidity was found to be positive, meaning that soil moisture increases with any rainfall events and increase in the air relative humidity. To better show the cross-correlation between the data streams, we also performed Pearson's correlation analysis following a time shift of the time series, aligning them to their respective time lags to achieve maximum correlation with soil moisture. The heatmap shown in Fig. 5 displays the Pearson's coefficient between soil moisture, air temperature, precipitation, counter radiation, relative humidity, soil heat flux, and global radiation.

3.2. Soil moisture prediction with deep learning

The point-scaled historical soil moisture data obtained from one sensor (F01) and the meteorological variables (*i.e.*, air temperature, precipitation, relative humidity, counter radiation, soil heat flux, and global radiation) collected from station 1 were used for model training and testing. The location of sensors and the original dataset obtained from the sensors are shown in Figs. 1 and 3, respectively. Each individual sensor data contains 62,103 datapoints collected at 10 min intervals for a period of 15 months (May 2021-July 2022). Furthermore, no data smoothing or noise reduction was preformed on the data to conserve the characteristics of the real-world data. We then used 75% of the soil and meteorological data for the ML model training and applied the following 25% for testing. The train set was used to build the forecast model and the test set was employed to evaluate the predictive performance of the built model by evaluating the performance metrics. After the model was built and its accuracy was tested, the performance of the model was evaluated to predict the soil moisture dynamics in different locations of the field using the data collected by other 28 soil sensors (F02-F29). The general workflow of the deep learning model implementation is depicted in Fig. 6.

The forecast lead time of the original LSTM model is 10 min. Forecast lead time represents the time interval between the current moment and the predicted moment. Fig. 7 depicts soil moisture dataset from sensor F01 splitting into training and testing sets to build the LSTM model. A long sequence (75%) of soil moisture data of sensor F01 (shown in Fig. 7) combined with meteorological variables (*i.e.*, air temperature, counter radiation, precipitation, relative humidity, soil

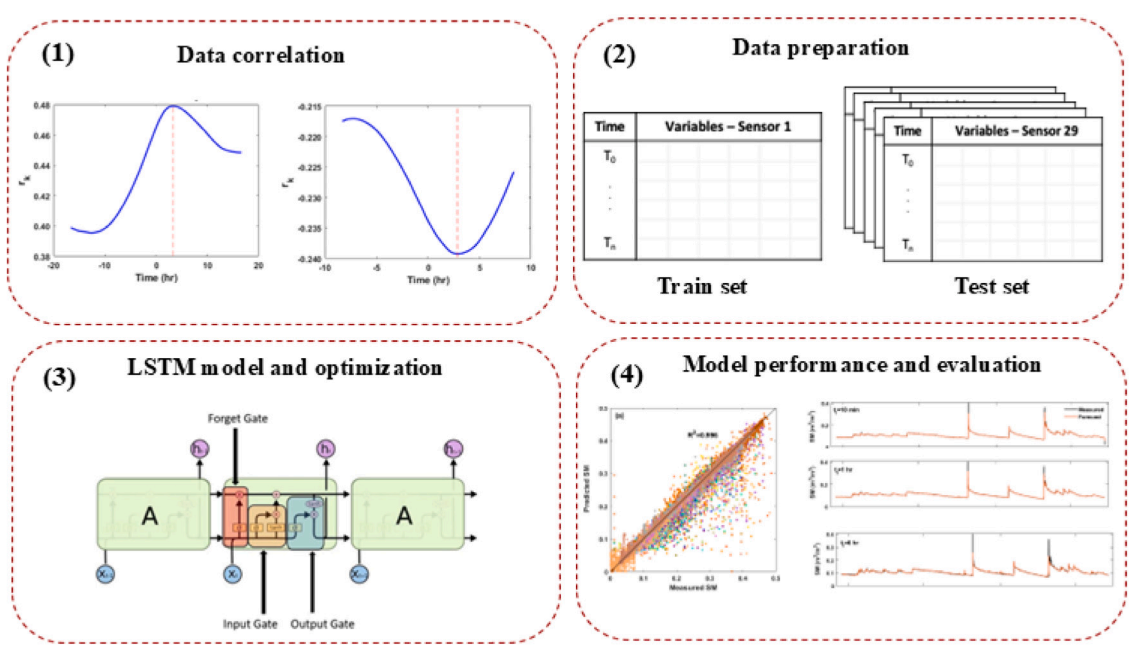

Fig. 6. General workflow used to build the deep learning model.

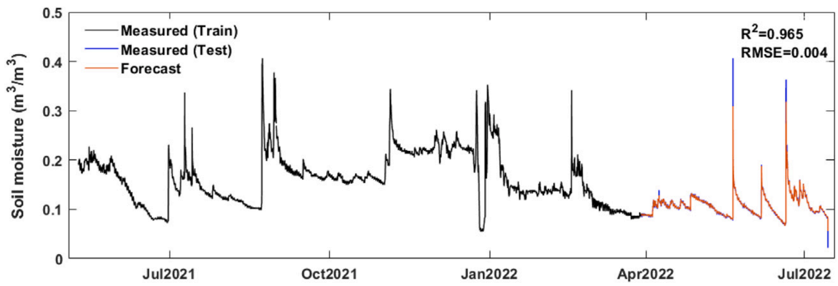

Fig. 7. Soil moisture data taken from sensor F01 used for training and testing the LSTM model.

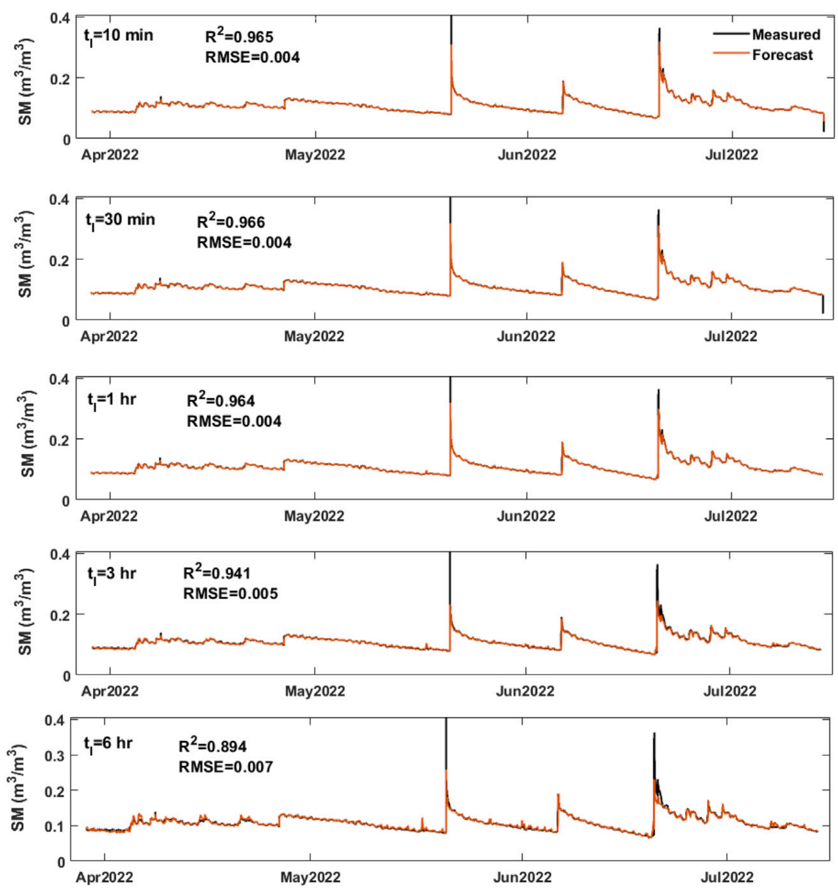

Fig. 8. Comparison between the measured and predicted soil moisture of sensor F01 for different lead times (t_l) for the test set.

heat flux, global radiation) were used to train the LSTM model. To evaluate the performance of the LSTM model, the predicted soil moisture values were compared with the reference soil moisture measurements for the test set (shown in Fig. 7). The close match between the forecast results and the ground truth values suggest that the developed model is capable of capturing the temporal patterns of SM for the 10 min lead time. The R^2 and RMSE values of the test set was found to be 0.965 and 0.004, respectively.

We further tested the prediction performance of the proposed model with different forecast lead times, namely, 30 min, 1 h, 3 h, 6 h, 12 h, and 24 h, using the soil moisture data of the sensor F01 and meteorological variables of station 1. It was found that the developed model represents an excellent prediction performance for the lead time up to 6 h. Fig. 8 compares the agreement between the predicted and observed SM values throughout the test period (April 2022–July 2022) for different forecast lead times including 30 min, 1 h, 3 h, and 6 h. It was observed that the ML model is capable of preserving the overall trend of the SM dynamics when different lead times were taken into account. However, the forecast performance slightly decreases with increasing forecast time (Babaeian et al., 2022; Zhang et al., 2018). The R^2 value of the test set for the 30 min, 1-h, 3-h, and 6-h lead times were 0.966, 0.964, 0.941, 0.894, respectively. Our results are comparable with the accuracy of the models developed in previous studies (Li et al., 2022; Obara and Nakamura, 2022). Table 1 reports the model evaluation results using different metrics across different lead times corresponding to the test set. From the practical perspective, the reduced accuracy for extended lead times may limit the efficacy of the prediction for agricultural and environmental management applications where long-term soil moisture content is necessary. To address this challenge, one may need to consider approaches such as transfer learning and ensemble techniques to accurately predict soil moisture for long time frames when limited training data is available (Obara and Nakamura, 2022; Datta and Faroughi, 2023).

To validate the performance of the developed LSTM model, the robustness of the model on prediction of soil moisture in other locations of the field was examined. For this purpose, we used the historical

Table 1
Predictive performance of the LSTM model for the test set across different lead times.

Lag time	R^2	$RMSE$	MAE	KGE
10 min	0.9655	0.0040	0.0009	0.9560
30 min	0.9665	0.0039	0.0009	0.9574
1 hr	0.9640	0.0041	0.0010	0.9482
3 hr	0.9414	0.0053	0.0017	0.8815
6 hr	0.8938	0.0071	0.0025	0.8321

data of soil moisture measured in sensors F02-F29 as well as the meteorological data as the input to the model that already built with the data of sensor F01. Fig. 9a depicts a cross-plot of the observed and predicted SM values at 28 different locations of the field when the lead-time was considered to be 10 min. As can be seen, the forecasts are close to the 1:1 line with the average R^2 value of 0.996, indicating that the LSTM model well captured the spatial variability of SM at the field scale. We further tested the model with different lead times on the prediction of SM in the locations of sensors F02-F29. The R^2 value obtained under different scenarios is representative of the suitable performance of the model for projection of SM for up to 6 h (Fig. 9b). However, the performance of the model for up to 24 h lead time has been shown in Fig. 9b. As shown, the median R^2 value decreased to 0.78 when the model was employed for prediction of soil moisture measured across all sensors, indicating a degradation in its predictive performance.

3.3. Practical implications and limitations

Prediction of soil moisture may have substantial significance for various stakeholders involved in agriculture, land management, and environmental planning. For instance, a model that can predict soil moisture dynamics is desirable for real-time irrigation scheduling. To achieve this using traditional modeling approaches, a deep understanding of vadose zone hydrology and atmospheric boundary layer is required. However, machine learning methods are strong tools for prediction of soil moisture dynamics as they can capture complex nonlinear relationship between the meteorological parameters, soil hydraulic properties, and the soil moisture dynamics. The LSTM model used in this study is a robust tool for prediction of soil moisture dynamics by preserving the historical trends in the soil moisture and climatic data. To optimize irrigation timing and volume in response to crop water needs, prediction of soil moisture dynamics is desirable for real-time irrigation scheduling. The model developed in this study is robust enough to provide short-term (one day ahead) prediction of soil moisture for independent sites in a large field that were not used in the model training. It is applicable to a case where the soil moisture needs to be predicted for irrigation purposes in a new site for which historical data to train an ML model is not available. Using a model already generated with historical data from another site, the prediction can be achieved with using the soil and climatic variables of the new site as inputs to the model. Prediction capability of the model for a rage of lead times has applications in a variety of practical agricultural scenarios. Short lead time predictions are applicable to real-time and high-frequency control in agricultural systems. However, longer lead time predictions can support tactical decision-making actions such as irrigation planning and equipment scheduling.

The developed LSTM model can be employed for real-time prediction of soil moisture in an area with a soil type similar to the location examined in this study. To improve the learning process in a long-term application and to adapt to new patterns of data stream and new soil and vegetation type, the deep learning model should be retrained periodically as new data are being acquired from sensors. Retraining should be determined by regularly evaluating the model's performance and considering factors that could affect its accuracy. According to the current study, feeding 1-year soil moisture and atmospheric data to the developed model for training is sufficient for the specific sensors deployed in the area of study, meaning that retraining the model may not be needed within one year. However, the training frequency should be determined according to the nature of the data streams, soil type, and land cover.

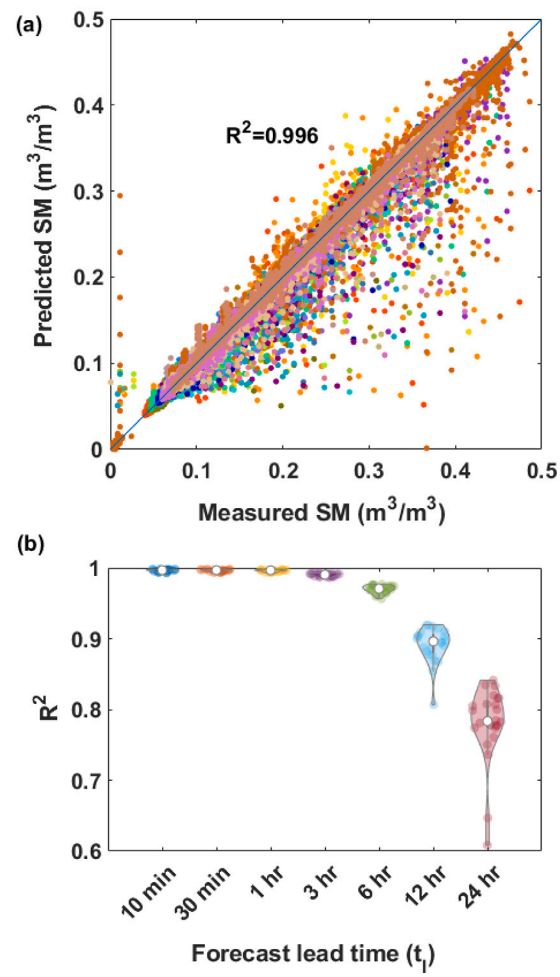

Fig. 9. (a) Scatter plot of measured and predicted soil moisture at different locations of the field, where sensors F02-F29 are located. Data covers the time period of May 2021–July 2022. The prediction lead time is 10 min. (b) Violin plots representing the variation of the prediction accuracy (R^2 score) of the LSTM model used for the prediction of soil moisture at locations of sensors F02-F29 with different lead times.

Forecasting soil moisture dynamics in response to precipitation events poses a challenge to LSTM-based models, especially when such events are underrepresented in the training data. While the developed model presents stronger performance during recession periods, it still provides satisfactory predictions during the precipitation events with capturing the overall trend and timing of soil moisture response. Despite the prediction limitations, the current model offers valuable predictive capability for operational lead times. Future studies could involve utilizing a training dataset with high-density rainfall events and incorporating features such as cumulative rainfall. Moreover, integrating physical constraints or attention-based architectures may help better capture the rapid dynamics. Li et al. (2019).

4. Conclusions

A deep learning neural network model based on LSTM networks and grid search (GS) optimization is proposed to predict field-scale soil moisture dynamics. The GS algorithm was used to optimize the

LSTM hyperparameters to improve the ability to learn data sequence features. To evaluate the performance of the proposed framework, we carried out more than a year long field-scale experiment in an area of approximately 20 hectare to measure a wide range of soil and climatic parameters. With its richness and granularity, this dataset was a valuable asset for training the ML model and instrumental to illustrate how the performance of the LSTM model's prediction changes at various forecast lead times. The measured data were used to develop quantitative models capable of predicting soil moisture dynamics in the field.

We demonstrated that a model trained using data collected from a single sensor in the field was capable of accurately predicting soil moisture dynamics across the entire field, with an impressive average R^2 value of 0.996 for a 10 min lead-time. This presents an excellent opportunity to reduce the need for extensive fieldwork for data collection in relatively homogeneous fields, resulting in notable savings of resources. To further this research, one could test the proposed methodology on broader areas, potentially utilizing data from satellite remote sensing. Therefore, the proposed methodology has the potential to significantly change the way soil moisture is monitored, leading to more efficient and effective farming practices and contribute to topics such as soil health and precision farming. Implementing such an approach to predict soil moisture dynamics on much larger scales would be a logical next step for this research.

CRediT authorship contribution statement

Sahar Bakhshian: Writing – review & editing, Writing – original draft, Visualization, Validation, Supervision, Software, Methodology, Investigation, Formal analysis, Data curation, Conceptualization. **Negar Zarepakzad:** Writing – review & editing, Writing – original draft, Visualization, Validation, Software, Methodology, Investigation, Formal analysis, Data curation. **Hannes Nevermann:** Writing – review & editing, Visualization, Methodology, Investigation, Formal analysis, Data curation. **Cathy Hohenegger:** Writing – review & editing, Resources, Methodology, Investigation, Funding acquisition, Conceptualization. **Dani Or:** Writing – review & editing, Visualization, Methodology, Investigation, Conceptualization. **Nima Shokri:** Writing – review & editing, Writing – original draft, Visualization, Validation, Supervision, Resources, Methodology, Investigation, Funding acquisition, Conceptualization.

Open research

The data from FESSTVaL (Field Experiment on submesoscale spatio-temporal variability in Lindenberg) campaign can be found in Hohenegger et al. (2023). The soil moisture data for all sensors are available under CC-BY 4.0 International license on Figshare (Bakhshian, 2024).

Declaration of competing interest

The authors declare that they have no known competing financial interests or personal relationships that could have appeared to influence the work reported in this paper.

Acknowledgments

The Max Planck Institute for Meteorology and Institute of Geo-Hydroinformatics at Hamburg University of Technology covered the costs of the soil sensors which is greatly appreciated. Nima Shokri would like to thank European Union's Horizon Europe research and innovation programme under grant agreement No.-101086179. The authors would like to acknowledge Dr. Frank Beyrich and Dr. Udo Rummel from Meteorological Observatory Lindenberg, The German Weather Service for providing us with the climatic data. This measurement was a part of FESSTVaL (Field Experiment on submesoscale spatio-temporal variability in Lindenberg) measurement campaign with several institutions involved whose contributions are acknowledged. Financial assistance was provided through the GAAC researcher grant to S.B. by the Bureau of Economic Geology (BEG), Jackson School of Geosciences, the University of Texas at Austin.

Data availability

The data from FESSTVaL (Field Experiment on submesoscale spatio-temporal variability in Lindenberg) campaign can be found in Hohenegger et al. (2023) Hohenegger et al. (2023). The soil moisture data for all sensors are available under CC-BY 4.0 International license on Figshare (Bakhshian, 2024) Bakhshian (2024).

References

Abbasimehr, H., Shabani, M., Yousefi, M., 2020. An optimized model using LSTM network for demand forecasting. Comput. Ind. Eng. 143, 106435. http://dx.doi.org/10.1016/j.cie.2020.106435, URL https://www.sciencedirect.com/science/article/pii/S0360835220301698.

Acharya, U., Daigh, A.L.M., Oduor, P.G., 2021. Machine learning for predicting field soil moisture using soil, crop, and nearby weather station data in the red river valley of the north. Soil Syst. 5 (4), http://dx.doi.org/10.3390/soilsystems5040057, URL https://www.mdpi.com/2571-8789/5/4/57.

Babaeian, E., Paheding, S., Siddique, N., Devabhaktuni, V.K., Tuller, M., 2022. Short- and mid-term forecasts of actual evapotranspiration with deep learning. J. Hydrol. 612, 128078. http://dx.doi.org/10.1016/j.jhydrol.2022.128078, URL https://www.sciencedirect.com/science/article/pii/S0022169422006539.

Bakhshian, S., 2024. Data_share.zip. http://dx.doi.org/10.6084/m9.figshare.25215752.v1.

Bakhshian, S., Romanak, K., 2021. DeepSense: A physics-guided deep learning paradigm for anomaly detection in soil gas data at geologic CO2 storage sites. Environ. Sci. Technol. 55, 15531–15541. http://dx.doi.org/10.1021/acs.est.1c04048.

Bengio, Y., Simard, P., Frasconi, P., 1994. Learning long-term dependencies with gradient descent is difficult. IEEE Trans. Neural Netw. 5 (2), 157–166. http://dx.doi.org/10.1109/72.279181.

Bergstra, J., Bengio, Y., 2012. Random search for hyper-parameter optimization. J. Mach. Learn. Res. 13, 281–305.

Brocca, L., Melone, F., Moramarco, T., Morbidelli, R., 2010. Spatial-temporal variability of soil moisture and its estimation across scales. Water Resour. Res. 46 (2), http://dx.doi.org/10.1029/2009WR008016.

Chen, X.-Y., Jin, Z.-G., 2012. Research on key technology and applications for Internet of Things. Phys. Procedia 33, 561–566. http://dx.doi.org/10.1016/j.phpro.2012.05.104, 2012 International Conference on Medical Physics and Biomedical Engineering (ICMPBE2012).

Datta, P., Faroughi, S.A., 2023. A multihead LSTM technique for prognostic prediction of soil moisture. Geoderma 433, 116452. http://dx.doi.org/10.1016/j.geoderma.2023.116452.

Dorigo, W., Wagner, W., Albergel, C., Albrecht, F., Balsamo, G., Brocca, L., Chung, D., Ertl, M., Forkel, M., Gruber, A., Haas, E., Hamer, P.D., Hirschi, M., Ikonen, J., de Jeu, R., Kidd, R., Lahoz, W., Liu, Y.Y., Miralles, D., Mistelbauer, T., Nicolai-Shaw, N., Parinussa, R., Pratola, C., Reimer, C., van der Schalie, R., Seneviratne, S.I., Smolander, T., Lecomte, P., 2017. *ESA CCI* soil moisture for improved earth system understanding: State-of-the art and future directions. Remote Sens. Environ. 203, 185–215. http://dx.doi.org/10.1016/j.rse.2017.07.001.

Entekhabi, D., Njoku, E.G., O'Neill, P.E., Kellogg, K.H., Crow, W.T., Edelstein, W.N., Entin, J.K., Goodman, S.D., Jackson, T.J., Johnson, J., Kimball, J., Piepmeier, J.R., Koster, R.D., Martin, N., McDonald, K.C., Moghaddam, M., Moran, S., Reichle, R., Shi, J.C., Spencer, M.W., Thurman, S.W., Tsang, L., Van Zyl, J., 2010. The soil moisture active passive (SMAP) mission. Proc. IEEE 98, 704–716. http://dx.doi.org/10.1109/JPROC.2010.2043918.

Géron, A., 2017. Hands-On Machine Learning with Scikit-Learn and TensorFlow. O'Reilly UK Ltd., Farnham.

Gers, F., Schmidhuber, J., Cummins, F., 2000. Learning to forget: continual prediction with LSTM. Neural Comput. 12 (10), 2451–2471. http://dx.doi.org/10.1162/089976600300015015.

Gupta, H.V., Kling, H., Yilmaz, K.K., Martinez, G.F., 2009. Decomposition of the mean squared error and NSE performance criteria: Implications for improving hydrological modelling. J. Hydrol. 377 (1), 80–91. http://dx.doi.org/10.1016/j.jhydrol.2009.08.003.

Hassani, A., Azapagic, A., Shokri, N., 2020. Predicting long-term dynamics of soil salinity and sodicity on a global scale. Proc. Natl. Acad. Sci. 117 (52), 33017–33027. http://dx.doi.org/10.1073/pnas.2013771117.

Hassani, A., Azapagic, A., Shokri, N., 2021. Global predictions of primary soil salinization under changing climate in the 21st century. Nat. Commun. 12, 6663. http://dx.doi.org/10.1038/s41467-021-26907-3.

Hengl, T., Mendes de Jesus, J., Heuvelink, G.B., Ruiperez Gonzalez, M., Kilibarda, M., Blagotić, A., Shangguan, W., Wright, M.N., Geng, X., Bauer-Marschallinger, B., Antonio Guevara, M., Vargas, R., MacMillan, R.A., Batjes, N.H., Leenaars, J.G.B., Ribeiro, E., Wheeler, I., Mantel, S., Kempen, B., 2017. SoilGrids250m: Global gridded soil information based on machine learning. PLoS One 12, e0169748. http://dx.doi.org/10.1371/journal.pone.0169748.

Hochreiter, S., Schmidhuber, J., 1997. Long short-term memory. Neural Comput. 9 (8), 1735–1780.

Hohenegger, C., Ament, F., Beyrich, o., 2023. FESSTVaL: The field experiment on submesoscale spatio-temporal variability in lindenberg. Bull. Am. Meteorol. Soc. 104 (10), E1875–E1892. http://dx.doi.org/10.1175/BAMS-D-21-0330.1.

Humphrey, V., Berg, A., Ciais, P., Gentine, P., Jung, M., Reichstein, M., Seneviratne, S.I., Frankenberg, C., 2021. Soil moisture–atmosphere feedback dominates land carbon uptake variability. Nature 592 (7852), 65–69. http://dx.doi.org/10.1038/s41586-021-03325-5.

Jiao, L., Yang, W., Jia, T., Maierdang, K., Chen, W., Gao, G., Wang, S., Liu, J., Wang, C., 2022. Effects of land use patterns on slope soil water in the semiarid loess plateau, China. J. Geogr. Sci. 32, 701–716. http://dx.doi.org/10.1007/s11442-022-1968-7.

Lehmann, J., Bossio, D.A., Kögel-Knabner, I., Rillig, M.C., 2020. The concept and future prospects of soil health. Nat Rev Earth Env. 1, 544–553. http://dx.doi.org/10.1038/s43017-020-0080-8.

Li, Q., Li, Z., Shangguan, W., Wang, X., Li, L., Yu, F., 2022. Improving soil moisture prediction using a novel encoder-decoder model with residual learning. Comput. Electron. Agric. 195, 106816. http://dx.doi.org/10.1016/j.compag.2022.106816.

Li, Y., Zhu, Z., Kong, D., Han, H., Zhao, Y., 2019. EA-LSTM: Evolutionary attention-based LSTM for time series prediction. Knowl.-Based Syst. 181, 104785. http://dx.doi.org/10.1016/j.knosys.2019.05.028.

Mahdaviara, M., Sharifi, M., Bakhshian, S., Shokri, N., 2022. Prediction of spontaneous imbibition in porous media using deep and ensemble learning techniques. Fuel 329, 125349. http://dx.doi.org/10.1016/j.fuel.2022.125349.

Nagaraj, P., Muneeswaran, V., Pallikonda Rajasekaran, M., Muthamil Sudar, K., Sumithra, M., 2021. Implementation of automatic soil moisture dearth test and data exertion using internet of things. In: Hassanien, A.E., Bhattacharyya, S., Chakrabati, S., Bhattacharya, A., Dutta, S. (Eds.), Emerging Technologies in Data Mining and Information Security. Springer Singapore, Singapore, pp. 511–517.

Oates, M., Fernández-López, A., Ferrández-Villena, M., Ruiz-Canales, A., 2017. Temperature compensation in a low cost frequency domain (capacitance based) soil moisture sensor. Agricult. Water. Manag. 183, 86–93. http://dx.doi.org/10.1016/j.agwat.2016.11.002, Special Issue: Advances on ICTs for Water Management in Agriculture.

Obara, Y., Nakamura, R., 2022. Transfer learning of long short-term memory analysis in significant wave height prediction off the coast of western Tohoku, Japan. Ocean Eng. 266, 113048. http://dx.doi.org/10.1016/j.oceaneng.2022.113048.

Or, D., Lehmann, P., Shahraeeni, E., Shokri, N., 2013. Advances in Soil Evaporation Physics—A Review. Vadose Zone J. 12 (4), http://dx.doi.org/10.2136/vzj2012.0163.

Reimers, N., Gurevych, I., 2017. Optimal hyperparameters for deep LSTM-networks for sequence labeling tasks. http://dx.doi.org/10.48550/ARXIV.1707.06799.

Seneviratne, S.I., Corti, T., Davin, E.L., Hirschi, M., Jaeger, E.B., Lehner, I., Orlowsky, B., Teuling, A.J., 2010. Investigating soil moisture–climate interactions in a changing climate: A review. Earth-Sci. Rev. 99 (3), 125–161. http://dx.doi.org/10.1016/j.earscirev.2010.02.004.

Shokri, N., Hassani, A., Sahimi, M., 2024. Multi-scale soil salinization dynamics from global to pore scale: A review. Rev. Geophys. 61, e2023RG000804. http://dx.doi.org/10.1029/2023RG000804.

Shokri, N., Or, D., Sahimi, M., 2012. Morphology, propagation, dynamics and scaling characteristics of drying fronts in porous media. Geophys. Res. Lett. 39, L09401. http://dx.doi.org/10.1029/2012GL051506.

Srivastava, N., Hinton, G., Krizhevsky, A., Sutskever, I., Salakhutdinov, R., 2014. Dropout: a simple way to prevent neural networks from overfitting. J. Mach. Learn. Res. 15 (1), 1929–1958.

Sun, S., Cao, Z., Zhu, H., Zhao, J., 2020. A survey of optimization methods from a machine learning perspective. IEEE Trans. Cybern. 50 (8), 3668–3681. http://dx.doi.org/10.1109/TCYB.2019.2950779.

Surakhi, O., Zaidan, M.A., Fung, P.L., Hossein Motlagh, N., Serhan, S., AlKhanafseh, M., Ghoniem, R.M., Hussein, T., 2021. Time-lag selection for time-series forecasting using neural network and heuristic algorithm. Electronics 10 (20).

Teshome, F.T., Bayabil, H.K., Schaffer, B., Ampatzidis, Y., Hoogenboom, G., 2024. Improving soil moisture prediction with deep learning and machine learning models. Comput. Electron. Agric. 226, 109414. http://dx.doi.org/10.1016/j.compag.2024.109414.

Topp, G.C., Davis, J.L., Annan, A.P., 1980. Electromagnetic determination of soil water content: Measurements in coaxial transmission lines. Water Resour. Res. 16 (3), 574–582. http://dx.doi.org/10.1029/WR016i003p00574.

Varshney, M., Singh, P., 2021. Optimizing nonlinear activation function for convolutional neural networks. Signal, Image Video Process. 15, 1323–1330. http://dx.doi.org/10.1007/s11760-021-01863-z.

Zhang, L., Cui, Y., Xiang, Z., Zheng, S., Traore, S., Luo, Y., 2018. Short-term forecasting of daily crop evapotranspiration using the 'Kc-ETo' approach and public weather forecasts. Arch. Agron. Soil Sci. 64 (7), 903–915. http://dx.doi.org/10.1080/03650340.2017.1387778.

Zhang, S., Shao, M., Li, D., 2017. Prediction of soil moisture scarcity using sequential Gaussian simulation in an arid region of China. Geoderma 295, 119–128. http://dx.doi.org/10.1016/j.geoderma.2017.02.003.